Microchemical Journal 170 (2021) 106666

Contents lists available at ScienceDirect

Microchemical Journal

journal homepage: www.elsevier.com/locate/microc

Molecularly imprinted solid-phase extractıon sorbent for selective determınatıon of melatonin

Elif Esen [a,*], Bilgen Osman [b], M. Nalan Demir [c]

[a] Dokuz Eylul University, The Graduate School of Natural and Applied Sciences, Department of Biotecnology, Izmir, Turkey
[b] Bursa Uludag University, Faculty of Arts and Science, Department of Chemistry, Bursa, Turkey
[c] Dokuz Eylul University, Faculty of Science, Department of Chemistry, Izmir, Turkey

ARTICLE INFO

Keywords:
Melatonin
Molecularly imprinted polymer
Solid phase extraction

ABSTRACT

In this study, melatonin (MLT)-imprinted poly (ethylene glycol dimethacrylate-N-methacryloyl-L-tryptophan methyl ester) [MLT-PEMATrp] microbeads were prepared for solid phase extraction (SPE) of melatonin (MLT) from edible plants prior to high performance liquid chromatography (HPLC) analysis. The microbeads were prepared via molecular imprinting technique by using MLT as a template. The MLT-PEMATrp microbeads were characterized by using Fourier transform infrared spectroscopy (FTIR), scanning electron microscopy (SEM), thermal gravimetic analysis (TGA), N_2 adsorption/desorption isotherms and swelling test. The parameters such as adsorption time, temperature, adsorbent amount, pH and ionic strength were detailedly optimized to increase the effciency of MLT adsorption procedure. The adsorption properties of MLT onto the MLT-PEMATrp microbeads (MIP) and non-imprinted PEMATrp microbeads (NIP) were investigated to show the effectiveness of imprinting. MIP showed higher adsorption capacity for MLT (Q_{MIP} = 207.71 mg g^{-1}) than NIP (Q_{NIP} = 12.15 mg g^{-1}). The relative selectivity coefficients calculated for serotonin (3.41) and L-tryptophan (5.94) indicated that MLT-PEMATrp microbeads exhibit significantly high selectivity for MLT. The microbeads were used for SPE of MLT from Linden (*Tilia tomentosa*), fennel (*Foeniculum Vulgare*), sage (*Salvia officinalis*) and chamomilla (*Matricaria chamomilla*) samples prior to HPLC analysis. The recoveries of MLT in the samples were in the range of 90–103.4%. The SPE method had a limit of detection (LOD) in the range of 0.026–0.094 μg mL^{-1}. The MLT-PEMATrp microbeads was very effective for SPE of MLT.

1. Introduction

Melatonin (N-acetyl-5-methoxytryptamine) (MLT), a small hyrophobic molecule, is a neurohormone secreted from the pineal gland and involves in various functions [1]. MLT is not only a mammalian product, it is also found in vertebrates, including algae and bacteria, in all non-mammal vertebrates, as well as in various plants [2]. Although MLT is an endogenously produced antioxidant, it can also be taken through foods [3,4]. MLT readily passes through the pinealocyte membrane and the capillary endothelium owing to its lipophilic nature and exhibits a wide range of antioxidant activity [5]. It has already been approved that MLT alleviates gastric ulcers and promotes gastric ulcer healing in patients with *H.Pylori* infections [6]. These protective actions involve numerous mechanisms such as increasing blood flow, sweeping free radicals, inhibiting matrix metalloproteinases (MMP)-3 and (MMP)-9, and reducing inflammation [7,8]. The therapeutic potential of MLT in gastric cancer cells has also been reported [9]. Many studies correlate the occurrence of disorders such as insomnia and neurodegenerative diseases to the decline of MLT hormone in the course of ages [10]. On the other hand, the role of MLT as a neuro-protective agent has been proposed for diseases such as Parkinson's and Alzheimer's, brain lesions caused by different etiologies such as ischemia and intracerebral hemorrhage [11,12].

Because of its therapeutic effects, MLT should be taken externally via synthetic MLT supplements, or natural sources including / producing MLT. It is also known that nutrients containing tryptophan such as strawberries, apples, cherries, fruit juices, rice, pistachio, almonds, spinach, cabbage, onions, tomatoes, cucumbers, flax seeds and sunflower seeds, herbal teas such as thistle, rye, fennel, sage and anise tea may increase the release of MLT in the body [13]. Therefore, the development of simple, precise and inexpensive methods for the determination of MLT amount in various samples such as edible plants and

* Corresponding author.
E-mail address: elifesen@outlook.com (E. Esen).

https://doi.org/10.1016/j.microc.2021.106666
Received 17 March 2021; Received in revised form 6 July 2021; Accepted 19 July 2021
Available online 27 July 2021
0026-265X/© 2021 Elsevier B.V. All rights reserved.

biological samples is of a great requirement.

Analytical methods used for the determination of MLT amount ranging from nanograms to picograms are radioimmunological assay (RIA) [14] enzyme-linked immunosorbent assay (ELISA) [15], high performance liquid chromatography (HPLC) and gas chromatography-mass spectrometry (GC–MS) with electrochemical and fluorescence detectors [16]. In the commercial RIA kits used together with a modified extraction procedure, however, interference of some chemicals such as calcium heparin is a problem in the analysis [17,18]. It has been determined that ELISA is a technically simpler method and the procedure can be applied by using smaller sample volumes. However, the method also requires an additional pre-concentration step to determine low levels of MLT [19]. In recent years, HPLC and GC–MS techniques have been used for quantitative determination of MLT, especially in tissue extracts [20]. However, the accuracy of quantitative analysis is low in the case that is difficult to separate all components in the mixtures. Thus, liquid–liquid extraction (LLE) [21], solid phase extraction (SPE) [22], solid–liquid extraction (SLE) [23] and ultrasonic extraction [24] are generally developed and used in the sample preparation stage. In comparison with other extraction methods, SPE comes to the fore due to the advantages such as high sample volume, high recovery, rapid sample loading and low organic solvent consumption. SPE cartridges can be prepared by using different polymeric adsorbents (polyaniline, styrene-methacrylate and styrene-N-vinylpyrrolidone copolymers, poly-N methylaniline (PNMA) and polydiphenylamine, polypyrrole (PPy), polymeric mixed mode anion exchanger (Oasis MAX, Waters) unmodified and hydroxylated polystyrene divinylbenzene polymers, styrene–divinylbenzene). Several SPE methods using commercial SPE adsorbents prior to instrumental analysis have been reported for MLT analysis. Commercial SPE adsorbents which are widely used for the SPE of MLT are C8 Amprep, C18, Strata-X, Waters Oasis HLB SPE cartridges [22,25,26]. However, separations used these common adsorbents in complex biological or environmental samples are not usually efficient due to their insufficient selectivity [27]. Therefore, it may be prefered to synthesize more selective adsorbents for SPE of MLT.

Recently, molecularly imprinted polymers (MIPs) have a great attention for SPE applications because of their superior characteristics such as stability, high specifity and recognition ability to a wide range of target molecules, relative ease and low cost of preparation [28,29]. MIPs are tailor-made polymeric materials synthesized in the presence of a template molecule to form complementary cavities after removal of the template [30]. MIPs have been commonly used as artificial receptors in sensors, catalysis, drug development and seperation. SPE is one of the most widely used application area due to the high potential of MIPs for commercialization. The increase in number of studies reporting the development of MIPs for SPE of different analytes [27,31] clearly demonstrates the usage potential of MIPs. To the best of our knowledge, there is no report on MLT preconcentration method in which MIPs used as a SPE adsorbent.

The main objective of the presented study is to investigate the effectiveness of melatonin (MLT)-imprinted poly (ethylene glycol dimethacrylate-N-methacryloyl-L-tryptophan methyl ester) [MLT-PEMATrp] microbeads as a SPE adsorbent before HPLC analysis. The MLT-PEMATrp microbeads were synthesized by suspension polymerization in the presence of MLT (template). N-methacryloyl-L-tryptophan methyl ester (MATrp) and ethylene glycol dimethacrylate (EGDMA) were a functional monomer and a crosslinker, respectively. The microbeads were characterized by Fourier transform infrared spectroscopy (FTIR), scanning electron microscopy (SEM), thermal gravimetric analysis (TGA), N_2 adsorption/desorption isotherm and swelling test. The effects of adsorbent amount, adsorption time, initial MLT concentration, pH, temperature and ionic strength on the adsorbed amount of MLT onto the MLT-PEMATrp microbeads were rigorously investigated. The microbeads were also used as a SPE adsorbent for selective preconcentration of MLT in linden (*Tilia Tomentosa*), fennel (*Foeniculum Vulgare*), sage (*Salvia Officinalis*) and chamomilla (*Matricaria Chamomilla*) samples before HPLC analysis. The plant samples were preferred since they have been widely consumed in Turkey due to their relaxing and therapeutic effects.

Table 1
Chromatographic conditions used for MLT analysis.

Apparatus	Thermo Scientific Dionex Ultimate 3000 LC System (Diode Array Sensor, Auto Sampler, Column Furnace)
Flow Rate (mL min^{-1})	1.000
Temperature (°C)	30
Injection Volume (μL)	20
Column	Thermo ODS-2-Hypersyl C18 (150 mm-4.6 mm-3 μm)
DAD Detector Wavelength (nm)	280
Manner of Work	Isocratic Elution
Mobile Phase	ACN:MeOH:0.5% Acetic Acid (60:30:10)
t_R (min)	1.80

2. Experimentals

2.1. Chemicals and reagents

The standard of MLT was obtained from Alfa Aesar (Kandel, Germany), Serotonin was obtained from Merck (Darmstadt, Germany) and L-tryptophan (L-Trp) were purchased from Sigma Chemical Co. (St. Louis, USA). Methanol (MeOH) and acetonitrile (ACN) were in HPLC grade and obtained from Sigma Aldrich. Poly(vinyl alcohol) (PVA) was supplied by Aldrich Chem. Co. (USA). EGDMA was obtained from Merck (Darmstadt, Germany), 2,2′-azobisisobutyronitrile (AIBN) was purchased from Fluka A.G. (Buchs, Switzerland). All other chemicals were of analytical grade. Water was produced with the Millipore ultra pure water device (Millipore Corporation (France) Elix 5® reverse osmosis unit, electrodisation (E.D.I) module (Elix 5® Water System), organic/colloid remover ion exchange system.

2.2. Apparatus

Chromatographic analysis of MLT was achived by Thermo Scientific Dionex Ultimate 3000 LC System (Diode Array Sensor, Auto Sampler, Column Furnace). Chromatographic conditions used for MLT analysis are summarized in Table 1.

2.3. Synthesis and characterization of MLT-PEMATrp microbeads

The following suspension polymerization procedure was applied for the preparation of MLT-PEMATrp microbeads. Firstly, a dispersion phase was prepared by dissolving a 0.2 g of PVA in 40 mL of distilled water. MATrp (functional monomer) and MLT (template) were mixed in the mole ratio of 1:1 and incubated overnight to prepare a pre-polymerization complex. The prepared pre-polymerization complex was added into a organic phase including EGDMA (5 mL) and toluene (7 mL) followed by a stirring period for 15 min at room temperature. Toluene was used as a diluent and a pore former in the polymerization procedure. After the addition of AIBN (0.1 g), the organic phase was poured into the dispersion phase in a closed cylindrical polymerization reactor. The mixture was polymerized for 4 h with a 150 rpm stirring rate at 65 °C. The resulted MLT-PEMATrp microbeads (MIP) were washed with an excess amount of ethanol and water to remove unreacted monomer residues. The template molecule (MLT) was removed by incubating the MLT-PEMATrp microbeads with 1 M NaCl solution until the MLT was not detected in desorption medium. The removal of MLT was followed by HPLC analysis. Finally, the microbeads were dried at 40 °C in a vacuum oven and used for the adsorption studies. The same polymerization procedure was applied to prepare non-imprinted PEMATrp microbeads (NIP) without addition of MLT. The reaction scheme for the polymerization is given in Fig. 1.

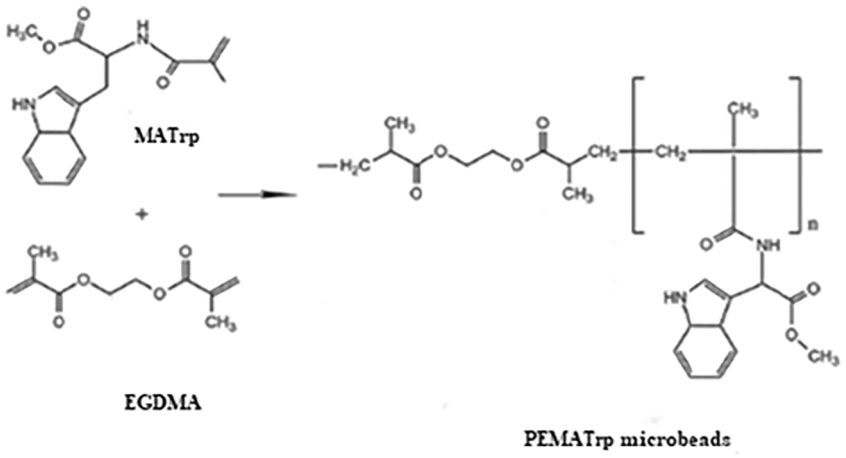


Fig. 1. Reaction scheme for MLT-PEMATrp synthesis.

The synthesized microbeads were characterized via SEM, FTIR, TGA, N_2 adsorption/desorption isotherm and swelling test. The physical morphology of the MLT-PEMATrp microbeads was observed via QUANTA 250 FEG scanning electron microscope after coating the microbeads with a gold film at an acceleration voltage of 3 kV. FTIR spectrum was recorded in the frequency range of 4000–400 cm^{-1} through a FTIR spectrometer equipped with an ATR sampling probe (Perkin Elmer, Spectrum 100). TGA analysis is one of the thermal analysis methods used to define the weight changes that may occur due to temperature in the sample. Thermal behavior of the MLT-PEMATrp microbeads was investigated via Perkin Elmer STA 6000 model thermogravimeter. During the TGA measurements, approximately 10 mg of sample was placed in a platinum crucible. Thermogravimetric analyses were performed at a heating rate of 10 °C min^{-1}, in the temperature range of 30–700 °C under nitrogen atmosphere with a flow rate of 2.0 mL min^{-1}. The specific surface area of the microbeads was determined by a multipoint Brunauer–Emmett–Teller (BET) apparatus (Quantachrome Corporation, Autosorb-6, USA). N_2 gas adsorption/desorption isotherm technique was used to measure the porosity of the MLT-PEMATrp microbeads (Quantachrome Corporation, Poremaster 60, USA). The BJH (Barrett, Joyner, Halenda) model was used to determine pore volume and pore size of the microbeads.

The swelling ratio of the microbeads was investigated by using the following procedure. Dry weight of the MLT-PEMATrp microbeads was recorded and then, the microbeads were kept in distilled water (2 mL) at 25 °C. After removal of excess water, the wet weight of the microbeads was carefully measured and the microbeads were tested by using the same procedure until the inflation equilibrium value was reached. The water absorbency (swelling equilibrium ratio), S_{eq}, was calculated using Equation (1).

$$\boldsymbol{Seq}\% = \frac{(\boldsymbol{Ws} - \boldsymbol{Wd})}{\boldsymbol{Wd}}\boldsymbol{x}100 \quad (1)$$

where W_s and W_d are the weights of the microbeads in the swollen and the dry states, respectively.

2.4. MLT adsorption and desorption studies

The effects of pH, adsorbent amount, contact time, initial MLT concentration, temperature and ionic strength were investigated in order to optimize the MLT adsorption onto MLT-PEMATrp microbeads. The effect of pH was evaluated in the pH range of 3.0–7.0 by using phosphate buffers for pH 6.0–7.0 and acetate buffers for pH 3.0–5.0. A 0.01 g of the microbeads was incubated with MLT solutions prepared at pHs ranging from 3.0 to 7.0. The initial concentration of MLT was 10 μg mL^{-1} with a volume of 5 mL. Different amounts of the MLT-PEMATrp microbeads (0.01–0.1 g) were incubated with MLT solutions (10 μg mL^{-1}, pH 4.0) to determine the effect of adsorbent amount. The effect of contact time was also investigated by incubating the microbeads (0.01 g) with MLT solution (initial concentration 10 μg mL^{-1} at pH 4.0) for 30 min and the samples were taken at different time intervals to determine the adsorbed amounts of MLT. The effect of the initial MLT concentration on the adsorption capacity of the MLT-PEMATrp microbeads was also studied. For this purpose, aqueous MLT solutions prepared at different MLT concentrations (1.0–300 μg mL^{-1}, pH 4.0) were incubated with the MLT-PEMATrp microbeads (0.01 g) at room temperature for 30 min. The adsorbed amounts of MLT were also evaluated in the temperature range of 15 °C to 60 °C. The ionic strength significantly affects the adsorption capacity. Therefore, the ionic strength of MLT solutions was changed by using NaCl solutions in the concentration range of 0.02 M to 0.1 M. The amount of the microbeads, initial MLT concentration and pH were 0.01 g, 10 μg mL^{-1} and 4.0, respectively. MLT solutions used in all experiments were prepared daily and kept under dark during experiments. The adsorbed amount of MLT onto the microbeads was calculated by considering the initial and final concentrations of the MLT solutions. The concentration of MLT was determined by HPLC analysis. Adsorption capacity of the MLT-PEMATrp microbeads, Q (mg g^{-1}), was calculated through Equation (2).

$$\boldsymbol{Q} = \frac{(\boldsymbol{C}_0 - \boldsymbol{C})\boldsymbol{V}}{\boldsymbol{m}} \quad (2)$$

where C_0, C, V, and m are the initial and final concentrations of MLT solutions (mg L^{-1}), volume of aqueous phase (L), and mass of the microbeads (g), respectively.

Desorption studies were conducted by using different desorption agents i.e, ethylacetate:MeOH (50:50), trietylamine:MeOH (50:50), acetic acid:MeOH (50:50) and 1 M NaCl. The MLT adsorbed microbeads (1 g) were incubated with the desorption agents (50 mL) at room temperature for 1 h. Desorption ratios for each desorption agent were calculated by using Equation (3).

$$\boldsymbol{Desorptionratio}(\%) = \frac{\boldsymbol{Desorbedamountof MLT}}{\boldsymbol{Adsorbedamountof MLT}}\boldsymbol{x}100 \quad (3)$$

The reusability of the MLT-PEMATrp microbeads was also investigated by using 1 M NaCl solution as a desorption agent. For this purpose, five adsorption–desorption cycles were performed under optimum conditions (pH: 4.0; initial MLT concentration: 10 μg mL^{-1}; solution volume: 5 mL; adsorbent amount: 0.01 g; time: 30 min, temperature: 25 °C).

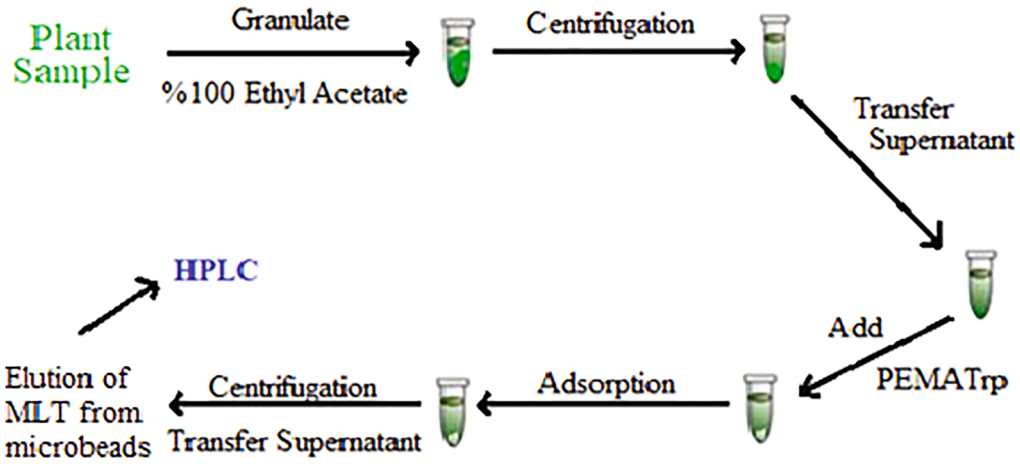


Fig. 2. MLT extraction procedure.

2.5. Selectivity studies

The selectivity of the MLT-PEMATrp microbeads was investigated under optimized conditions by using L-Trp and serotonin as competitor molecules (competitor concentration: 10 μg mL^{-1} solution volume: 5 mL; pH: 4.0; time: 30 min; adsorbent amount: 0.01 g; temperature: 25 °C). The mobile phase ratios used for HPLC analyses were ACN: MeOH:0.5% acetic acid (60:30:10) for L-Trp and ACN:MeOH:0.5% acetic acid (45:45:10) for serotonin, respectively. The distribution coefficients were calculated by Equation (4).

$$K_d = \frac{C_i - C_f}{C_f} \times \frac{V}{m} \quad (4)$$

where K_d is the distribution coefficient (mL g^{-1}); C_i is the initial and C_f is the final concentration (mg L^{-1}) of adsorbate molecules (MLT, L-Trp and serotonin); m is the amount of polymer used (g) and V is the volume of the solution (mL).

The selectivity coefficient (k) was calculated through Equation (5) where K_{dMLT} and K_{dX} are the distrubion coefficients for MLT and competitor molecules (L-Trp or seratonin), respectively.

$$k = \frac{K_{dMLT}}{K_{dX}} \quad (5)$$

In addition, the relative selectivity coefficient (k') was calculated from Equation (6).

$$k' = \frac{k_{MIP}}{k_{NIP}} \quad (6)$$

where k_{MIP} and k_{NIP} are selectivity coefficients calculated for the MIP and NIP, respectively.

2.6. MLT analysis in plant samples

Linden (*Tilia tomentosa*), fennel (*Foeniculum Vulgare*), sage (*Salvia officinalis*) and chamomilla (*Matricaria chamomilla*) samples were used for MLT analyses. Firstly, the plant extracts were prepared by using the following procedure. Briefly, 12 mL of the extraction solvent (ethyl acetate) was added to the plant sample (2 g) and the mixture was milled for 3–4 min. The sample was kept at room temperature for 2 h. Then, the sample was centrifugated at 10000 rpm for 15 min and the supernatant was used for HPLC analysis. 5 mL of the plant extract was incubated with a 0.01 g of the MLT-PEMATrp microbeads for 30 min (pH 4.0, 25 °C). Adsorbed MLT was eluted by washing the microbeads with a 5 mL of 1 M NaCl (desorption agent) for 1 h and the eluent was analyzed by HPLC. The MLT extraction procedure is summarized in Fig. 2.

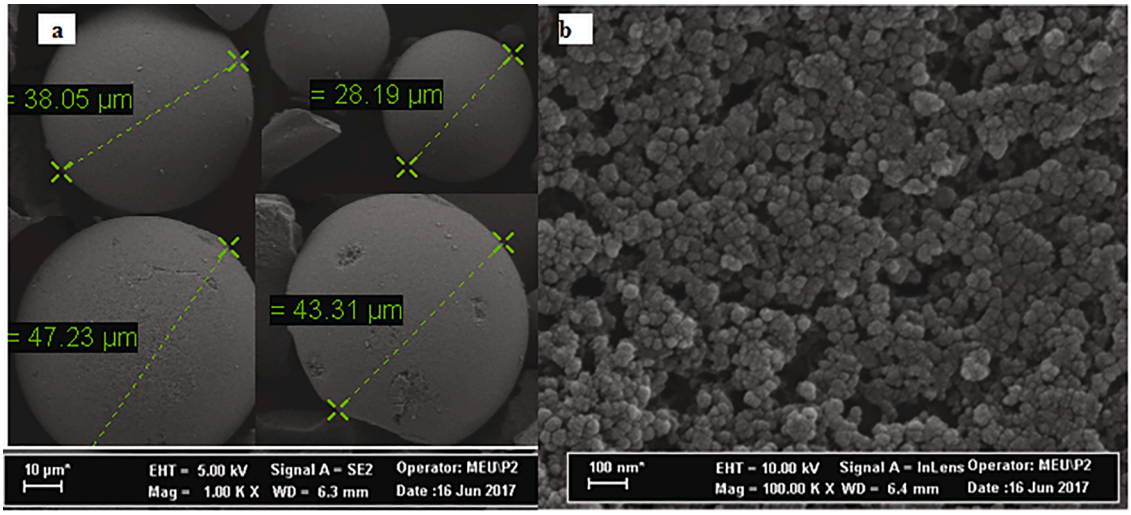


Fig. 3. SEM images of the MLT-PEMATrp microbeads.

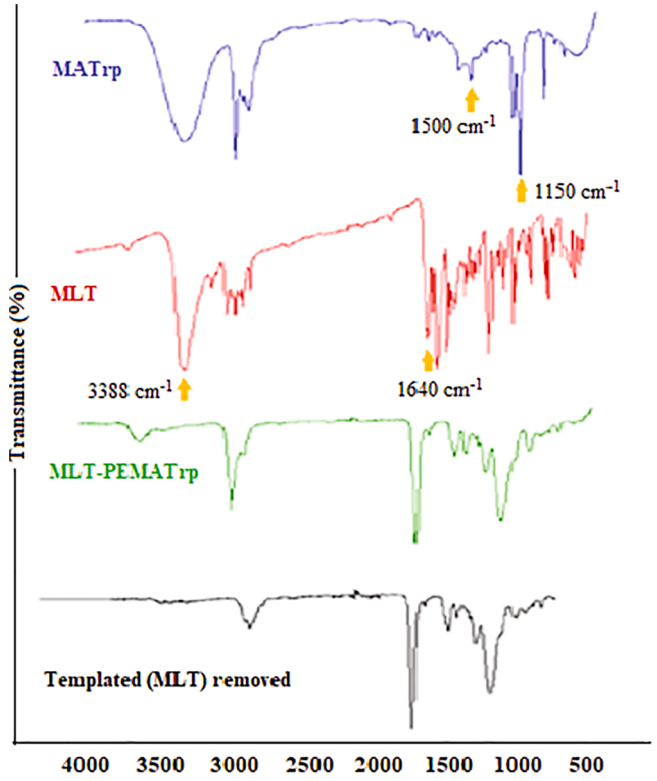


Fig. 4. FTIR spectra of MATrp (blue), MLT (red), MLT-PEMATrp microbeads (green) and MLT-PEMATrp microbeads after template (MLT) removal (black). (For interpretation of the references to colour in this figure legend, the reader is referred to the web version of this article.)

3. Results and discussion

3.1. Properties of the MLT-PEMATrp microbeads

The MLT-PEMATrp microbeads were synthesized via suspension polymerization technique to obtain polymers in spherical form. The physical morphology of the microbeads was visualized through a SEM analysis. The SEM images presented in Fig. 3 clearly show that the applied polymerization procedure enabled to obtain polymers in spherical form. The polymeric microbeads can swell in aqueous medium due to the covalent crosslinks. The swelling ratio of the MLT-PEMATrp microbeads was determined as to 220%, which is an advantage for adsorption studies in aqueous medium.

The chemical characterization of the microbeads was conducted via FTIR analysis. The FTIR spectra for MATrp, EGDMA, MLT and the MLT-PEMATrp microbeads were recorded and the resulting spectra are depicted in Fig. 4. When the FTIR spectra of MLT, MATrp and MLT-PEMATrp microbeads were examined, it was observed that MLT bands were also present in the spectrum of the microbeads. The broad band at 3388 cm^{-1} indicates the amine group (N–H aromatic) in the indole structure. The absorption bands at about 3000 cm^{-1} and 900 cm^{-1} were resulted from the aromatic C–H bending vibration of the indole ring in MLT and MATrp. The band at 1640 cm^{-1} shows the existence of C═O groups in the MLT molecule. The band belonging to C═O groups in EGDMA structure is also observed at 1757 cm^{-1}. The absorption bands observed at 1150 cm^{-1} and at around 1500 cm^{-1} correspond to the ester group of the MATrp (C-O stretching) and C═C groups in aromatic ring of MATrp, respectively. It is important to demonstrate the presence of MLT in the imprinted sorbent and the removal of the template (MLT) from the sorbent in the given FTIR spectra. It is shown that most of the important absorption bands observed in the FTIR spectrum of the polymer become weaker drastically after the MLT template was removed.

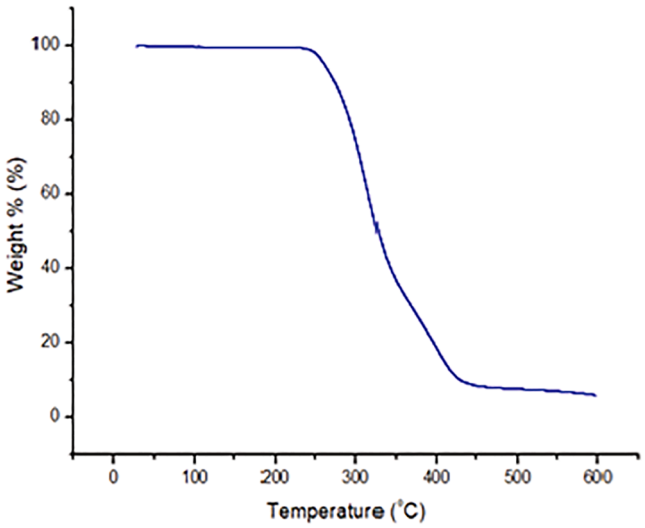


Fig. 5. TGA curve of the MLT-PEMATrp microbeads.

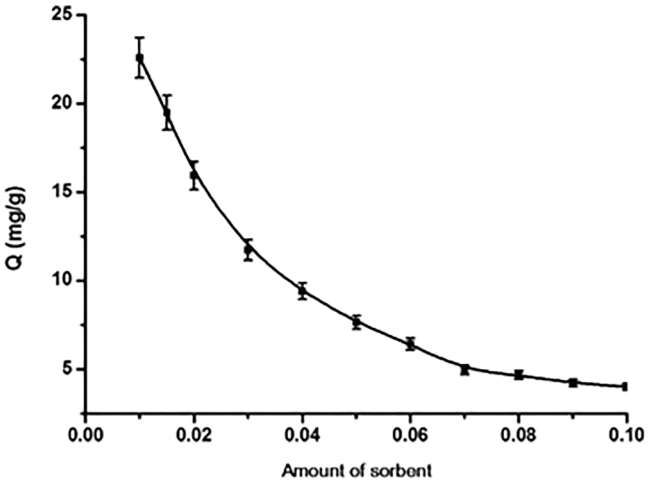


Fig. 6. Effect of adsorbent amount on MLT adsorption.

Thermal degradation behaviour of the MLT-PEMATrp microbeads was investigated by TGA analysis in the temperature range of 30–700 °C under nitrogen atmosphere. TGA curve depicted in Fig. 5 clearly shows that the the degradation of the microbeads occured in two stages of mass loss: the first was observed at a temperature lower than 200 °C while the other was determined at a temperature higher than 300 °C. The first mass loss was around 50 °C due to loss of adsorbed water and other volatile impurities. The highest mass loss was detected in second stage at a temperature around 420 °C probably resulting from the decomposition of polymer matrix. The mass loss of MLT-PEMATrp microbeads was 97.8%. The remaining portion, which is 2.2%, belongs to inorganic residuals.

The BET surface area and pore volume of the MLT-PEMATrp microbeads were determined as 400.2 $m^2\ g^{-1}$ and 0.9798 $cm^3\ g^{-1}$, respectively. The N_2 adsorption/desorption isotherm and pore diameter distribution curve is given in Supporting Information (Fig SI1). The MLT-PEMATrp microbeads were found to be type IV isotherm according to IUPAC classification. Pore diameters changing in the range of 1.03 nm (micro) to 17.53 nm (meso) showed that the microbeads contain both micropores and mesopores.

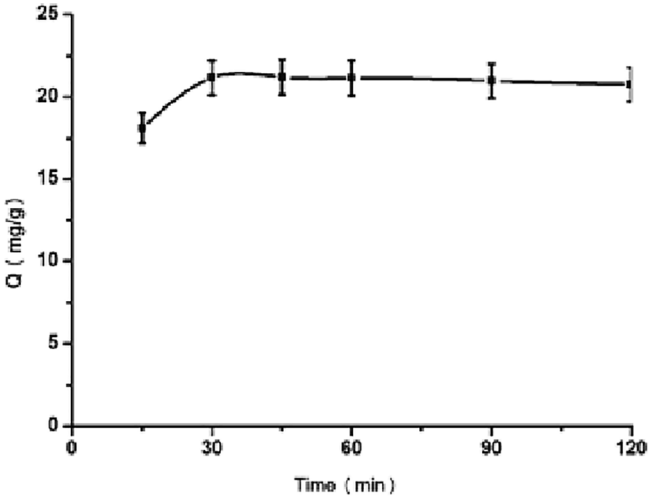


Fig. 7. Effect of contact time on MLT adsorption.

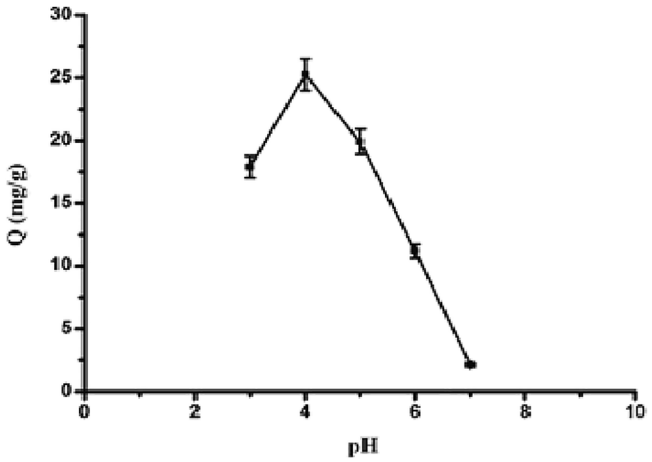


Fig. 8. Effect of pH on MLT adsorption.

3.2. Adsorption studies

The effects of contact time, initial MLT concentration, pH, adsorbent amount, temperature and ionic strength were investigated to optimize MLT adsorption process, In order to determine the effect of the adsorbent amount, 5 mL of 10 μg mL^{-1} MLT solution was treated with different amounts of adsorbent (0.01–0.1 g) at 25 °C for 30 min at pH 4.0. At high adsorbent amounts, binding sites in the MLT-PEMATrp microbeads were not fully saturated with MLT and thus, the adsorption capacity (Q, mg MLT g^{-1} microbeads) decreased (Fig. 6). When the adsorbent amount was 0.01 g, adsorption capacity was reached the highest value. This result showed that the affinity of the MLT-PEMATrp microbeads to MLT is very high, which is an advantage for SPE of MLT from real samples.

Fig. 7 shows the effect of contact time on the adsorbed amount of MLT onto the microbeads. It was clear that the adsorption was very fast (30 min) ensuring a rapid SPE of MLT.

The maximum MLT adsorption on the MLT-PEMATrp microbeads occured at pH 4.0 (Fig. 8). The photolysis of MLT in aqueous solution has been studied spectrometrically with a 248 nm laser (Fig. 9) [32]. Although, the pKa values for MLT were 1.2 and 12.7 in aqueous solution, the big difference for the relative intensity of the absorption peaks under various pH conditions reveals that the MLT radical exists in the solution through an acid–base equilibrium. In support from the pH dependence of the spectrum of the intermediate, the pKa_1 for the doubly-protonated MLT radical against the mono-protonated MLT cation radical was estimated to be − 0.95 and the pKa_2 for the mono-protonated MLT cation and MLT neutral radical was 4.5 ± 0.5.

Additionally, a stability study of mel MLT atonin at different pH values was done in aqueous media via UV–Vis spectrophotometry, which reveals that at acidic pH MLT is unstable when interacting with the environment (light and oxygen) [33]. The dominant forces in physical adsorption are secondary interactions such as hydrogen bonds, dipole–dipole interactions, electrostatic interactions, van der Waals interactions, hydrophobic interactions. It is difficult to decide the type of intermolecular interactions in MLT adsorption onto the MLT-PEMATrp microbeads. Because the environmental conditions such as light and oxygen effects the molecular properties of MLT even if the experimental conditions were designed to restrain the effects of light and oxygen. It can be considered that the decrease in the adsorption capacity at pH values below and above pH 4.0 may result from the electrostatic repulsion.

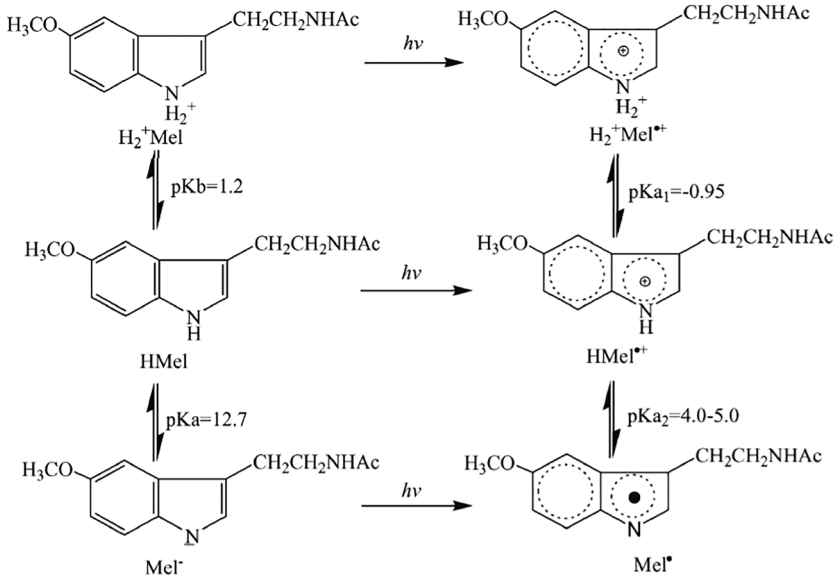


Fig. 9. Photolysis study of MLT with 248 nm laser light [32]

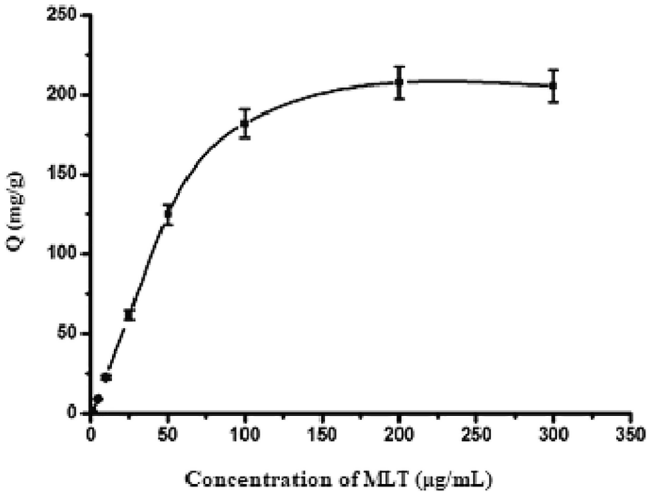


Fig. 10. Effect of initial MLT concentration on MLT adsorption.

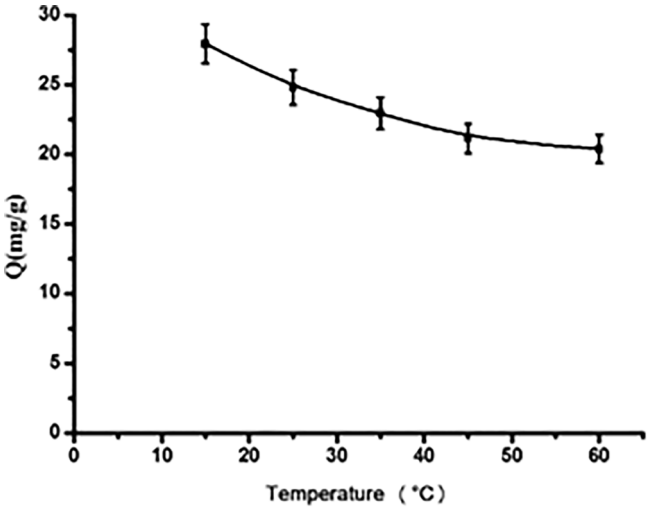


Fig. 11. Effect of temperature on MLT adsorption.

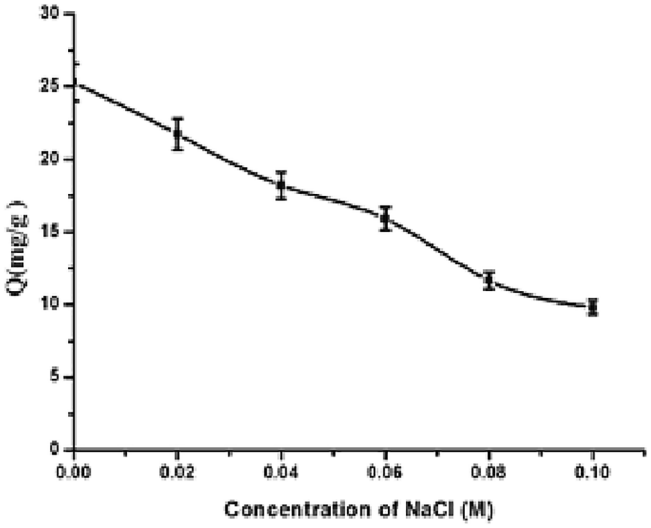


Fig. 12. Effect of ionic strength on MLT adsorption.

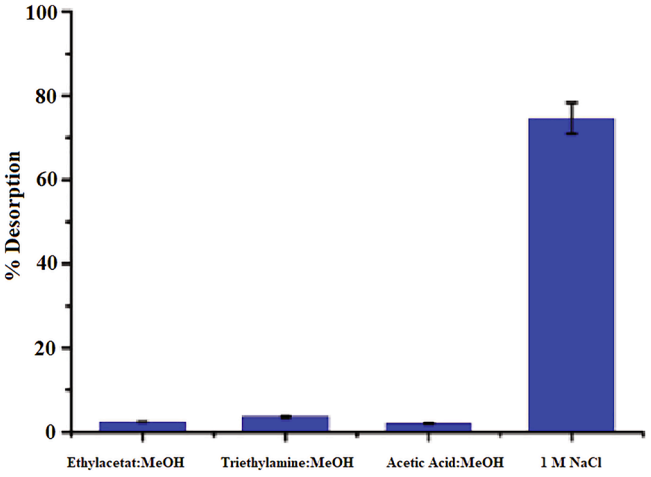


Fig. 13. Desorption of MLT from the MLT-PEMATrp microbeads.

The effect of initial MLT concentration on the adsorbed amount of MLT is depicted in Fig. 10. The adsorbed amount of MLT was increased with increasing MLT concentration from 1 to 300 µg mL^{-1} and it was reached to an equilibrium value at about 100 µg mL^{-1} initial MLT concentration. Maximum adsorption capacities were found to be 207.71 mg g^{-1} for MIP and 12.15 mg g^{-1} for NIP, respectively. Adsorption capacity of the MIP was about 5 times higher than that of NIP.

When the temperature increased from 15 °C to 60 °C, the adsorbed amount of MLT onto MLT-PEMATrp microbeads decreased by 27.02% (Fig. 11). El Moussaoui et al., showed that concentration of MLT standard stored at four different temperatures (–32, 4, 25 and 50° C) under exposure to light for 15 days resulted in high degradation at up to 16%, 17%, 22%, and 22%, respectively and that the concentration of MLT in solutions kept at room temperature (25 °C) under exposure to light and air significantly decreased to 43% [34]. On the other hand, Zafra-Roldan et al. showed that MLT in acidic pH solution (25 °C) was stable when protected from the environment [33]. Hence, it can be said that temperature may not be the most important variable for MLT degradation. Consequently, the decrease observed in the adsorption capacity with increasing temperature demonstrated the exothermic nature of MLT adsorption.

The ionic strength significantly effected the adsorption capacity of MLT-PEMATrp microbeads (Fig. 12). When the NaCl concentration in the adsorption medium was increased from 0.02 M NaCl to 0.1 M NaCl (pH:4.0), the adsorbed amount of MLT decreased by 18%. The results

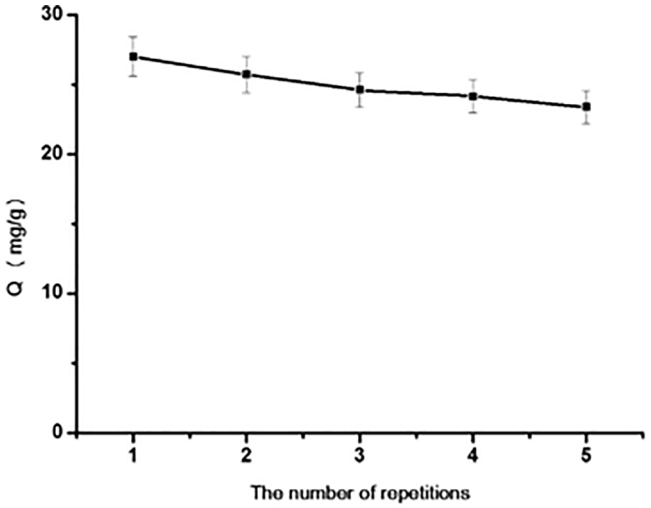


Fig. 14. Reusability of the MLT-PEMATrp microbeads.

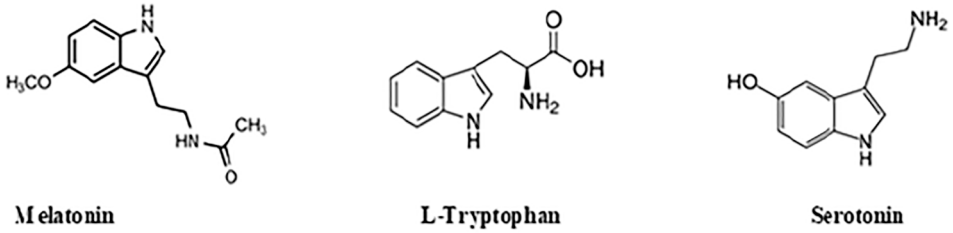


Fig. 15. Chemical structures of MLT, L-Trp and serotonin.

Table 2
The distribution coefficients, selectivity coefficients and relative selectivity coefficients.

	MIP		NIP		
	K_d (mL g^{-1})	*k*	K_d (mL g^{-1})	*k*	*K'*
MLT	10.15	–	3.07	–	–
Seratonin	2.38	4.26	2.45	1.25	3.41
L-Trp	2.71	3.74	4.86	0.63	5.94

gave rise to thought that the interaction between MLT and MLT-PEMATrp microbeads can be electrostatic. At higher ionic strength, the interaction between the MLT molecules and adsorbent decreased since Na^+ and Cl^- ions interacted with the charged groups of MLT and MLT-PEMATrp polymer resulting in a decrease in their net charges. Although MLT has no ionizable groups in the studied pH range, pH changes strongly effected the adsorption capacity of the MLT-PEMATrp microbeads supporting that the interaction may be electrostatic due to MLT unstability.

3.3. Desorption and reusability studies

The efficiencies of different desorption agents were rigorously investigated (Fig. 13). The results showed that 1 M NaCl was the most effective desorption agent with a desorption ratio of 85% at only 1 h. When 1 M NaCl solution was used as a desorption agent in the adsorption–desorption cycles which were repeated five times, it was detected that the decrease in adsorption capacity of the MLT-PEMATrp microbeads was very low (14%) (Fig. 14).

3.4. Selectivity of the MLT-PEMATrp microbeads

To determine the selectivity of the MLT-PEMATrp microbeads, adsorption studies were conducted using L-Trp and serotonin as competitor molecules under optimized conditions (adsorbent amount: 0.1 g, pH: 4.0, time 30 min, temperature: 25 °C). These compounds were preferred as competitor molecules due to their structural similarity to MLT. The chemical structures of MLT, L-Trp and serotonin are given in Fig. 15.

MLT solution (10 μg mL^{-1}) and competitor solutions (10 μg mL^{-1} each) were separately interacted with the MIP and NIP. The adsorbed amounts were determined and calculated distribution coefficients (K_d), selectivity coefficients (k) and relative selectivity coefficients (k′) are depicted in Table 2.

The K_d values of competitor molecules for the MIP (2.38 mL g^{-1} for serotonin and 2.71 mL g^{-1} for L-Trp) were lower than those for the NIP (2.45 mL g^{-1} for serotonin and 4.86 mL g^{-1} for L-Trp) demonstrating that the binding cavities in the MLT-PEMATrp microbeads have no specificity for these molecules. In addition, K_d of MLT for the MIP (10.15 mL g^{-1}) was evidently higher than that of MLT for the NIP (3.07 mL g^{-1}). These results indicated that selective binding sites were successfully formed into the MLT-PEMATrp microbeads. The relative selectivity coefficients (k′) for serotonin and L-Trp were 3.41 and 5.94, respectively (Table 2). High relative selectivity coefficients also demonstrated that the MIP microbeads have a high affinity for MLT.

Table 3
Results for plant samples.

Plant Sample	Spiked MLTconcentration (μg mL^{-1})	Found (μg mL^{-1})	Recovery (%) ± RSD
Linden	2.50	2.56	99.6 ± 0.55
	5.00	4.86	97.3 ± 0.70
	10.00	10.07	101.3 ± 0.57
Fennel	2.50	2.51	98.9 ± 0.45
	5.00	5.07	101.6 ± 1.22
	10.00	10.18	103.4 ± 0.97
Sage	2.50	2.27	90.7 ± 0.57
	5.00	5.14	102.2 ± 0.23
	10.00	10.1	100.4 ± 0.61
Chamomilla	2.50	1.94	90.0 ± 0.49
	5.00	5.16	91.9 ± 0.18
	10.00	10.11	100.5 ± 0.19

3.5. SPE of MLT in plant samples

The MLT-PEMATrp microbeads were used as adsorbent for SPE of MLT from linden (*Tilia Tomentosa*), fennel (*Foeniculum Vulgare*), sage (*Salvia Officinalis*) and chamomilla (*M.Chamomilla*) samples purchased from local markets in Izmir/TURKEY. SPE procedure was applied under the optimized conditions (adsorbent amount: 0.1 g, pH: 4.0, time 30 min, temperature: 25 °C). The plant samples were spiked with MLT at different concentrations for the evaluation of the accuracy of the developed method. The results are summarized in Table 3. The recoveries % of MLT in plant samples were in the range of 90 to 103%. The recoveries of the developed method in this study are very high and within acceptable limits.

3.6. Method validation

The limit of detection (LOD), limit of quantification (LOQ) and analytical performance parameters of the optimized SPE method are given in Table 4. LOD and LOQ were calculated using two different formulas (LOD = 3.3 S/m and LOQ = 10 S/m) by measuring the response of lowest concentration that could be measured. The calculations are based on standard deviation of signals of the lowest concentration of the analyte (S) and slope of the calibration curve (m). Intra-day precision, was calculated as relative standard deviation % (RSD %) by analysis of five replicates and the inter-day precision was obtained by analysing samples in seven different days, at two spiked concentration levels, 2.5 μg mL^{-1} and 10 μg mL^{-1}.

The intra-day relative standard deviations (RSD %) were determined as lower than 0.95% by analysing samples five measurements taken on the same day. Moreover, inter-day RSD % values were determined as lower than 0.76 % by analysing samples in seven different days. The results shown in Table 4 well demonstrated that the developed method possesses low LOD and LOQ, good precision and can be employed to quantify low contents of MLT in plant samples.

The SPE method for MLT determination is rarely reported in the literature. In addtion, there is no study reporting the development and

Table 4
Analytical performance parameters.

PlantSample	Calibration Equation	Correlation Coefficient (R^2)	DynamicRange(μg mL^{-1})	LOD(μg mL^{-1})	LOQ(μg mL^{-1})	Intra-day assay(RSD,%) *Spiked (μg mL^{-1})2.5 10	Inter-day assay(RSD, %) *Spiked (μg mL^{-1})2.5 10
Linden	y = 0.2827x + 109.9	0.9961	2.5–50	0.026	0.079	0.52 0.59	0.05 0.43
Fennel	y = 0.2505x + 188.3	0.9917	1–100	0.057	0.174	0.43 0.95	0.40 0.76
Sage	y = 0.3358x + 115.1	0.9934	1–100	0.031	0.092	0.55 0.63	0.50 0.49
Chamomilla	y = 0.4246x + 104.6	0.9904	1–100	0.094	0.287	0.51 0.22	0.40 0.11

* Spiked concentrations in 2.5 and 10 μg mL^{-1}.

Table 5
Comparison of the proposed method with other methods reported in the literature for MLT.

Analytical Method	Sample Preparation	Matrix	Solid phase (mg)	LOD	LOQ	Recovery (%)	RSD(%)	Analysis time (min)	Refs.
HPLC-DAD	US-DLLME	Wine	–	0.23 μg L^{-1}	0.70 μg L^{-1}	92–103	0.8–1.9	5.0	[21]
HPLC-FD	SPE	Wine	200–500	0.075 μg mL^{-1}	0.25 μg mL^{-1}	26–110	–	–	[35]
HPLC-ECD	SPE	Cherry	60	0.025 μg mL^{-1}	0.025 μg/mL	74–91	–	15	[36]
CD-MEKC	SPE	Plants	500	0.79 ng g^{-1}	0,0262 ng g^{-1}	108–87	2.30	10	[22]
HPLC-PDA	SPE	Water	50	0.026 μg mL^{-1}	0.078 μg mL^{-1}	100.5	1.25	1.3	[37]
HPLC-UV	DSPE	Food	–	0.10 μg mL^{-1}	0.40 μg mL^{-1}	91.5–109.6	1.1–1.7	11	[38]
HPLC-DAD	**SPE**	**Plants**	**10**	**0.026** μg mL^{-1}	**0.079** μg mL^{-1}	**90.7–103.4**	**0.18–1.22**	**1.8**	**This work**

HPLC-DAD: High-performance liquid chromatography-diode array detection, HPLC-ECD: High-performance liquid chromatography-electrochemical, CD-MEKC: Cyclodextrin-modified micellar electrokinetic chromatography, HPLC-UV: High-performance liquid chromatography-ultraviole detection, HPLC-FD: High-performance liquid chromatography-fluorescence detector, HPLC-PDA: High-performance liquid chromatography- equipped with photodiode array detector, DSPE: Dispersive SPE, US-DLLME: Ultrasound-dispersive liquid–liquid microextraction.

usage of MIPs for SPE of MLT. In a study reporting the development of a SPE method using octadecylcilica (C18) (500 mg, adsorbent amount) and poly(styrene–divinylbenzene) (DVB) (200 mg, adsorbent amount) commercial cartridges for MLT determination in wine samples via HPLC analysis, LOD was found 0.075 μg mL^{-1} which was similar to LOD in this study [35] Similarly, SPE methods were used for analysis of MLT in cherry (DVB and HLB commercial cartridges) [36] plants (C8 commercial cartridge) [22] and water (poly(lactic acid) nanoparticles) [37]. The parameters of other methods such as amounts of solid phases, LOD, LOQ, recovery %, RSD % are summarized in Table 5 enabling the comparison of the proposed method with other methods reported in the literature. It is clearly seen that the amount of solid phase (MLT-PEMATrp microbeads) was considerably lower than those of commercial cartridges. By the way, the LOD/LOQ, recovery %, RSD % values are comparable with other methods. The results indicated that the developed SPE method can be used efficiently for the fast determination of MLT with a small amount of adsorbent (10 mg).

4. Conclusion

MIPs have been successfully used as SPE sorbents for extraction and selective determination of analytes from different samples, such as environmental, biological, food, drug and other real samples because of their advantages, including high selectivity, stability, reusability and low cost. In this study, MLT-PEMATrp microbeads were used as an affinity sorbent in SPE of MLT in plant samples prior to HPLC analysis. Parameters affecting the MLT adsorption such as adsorbent amount, contact time, initial MLT concentration, temperature, pH and ionic strength were detailedly optimized. It was determined that MLT adsorption could be performed with only 10 mg of microbeads. MLT adsorbed onto the MLT-PEMATrp microbeads was desorbed with 1 M NaCl by 85% in 1 h and it was indicated that the microbeads can be used repeatedly. The high relative selectivity coefficients (k′) clearly demonstrated the selectivity of the microbeads. The microbeads were also successfully used for SPE of MLT in edible plant samples by HPLC analysis. Recoveries were 97%, 96% and 95% for linden, fennel and sage, respectively, demonstrating the validity of the developed SPE method with a good linearity ($R^2 \geq 0.9904$) and a repeatability (RSD% $\leq$ 1.22). The developed method possesses low LOD and LOQ, good precision, it can be employed to quantify low contents of MLT in plant samples. Consequently, a new and cost effective SPE method enabling the rapid determination of MLT with a low amount of adsorbent was successfully developed. It can be said that the synthesized MLT-PEMATrp microbeads can be applied in biotechnological studies and have the economical advantage for large-scale applications.

Declaration of Competing Interest

The authors declare that they have no known competing financial interests or personal relationships that could have appeared to influence the work reported in this paper.

Acknowledgement

This work was supported by the Department of Scientifict Research Project of Dokuz Eylul University (Grant No: 2016.KB.FEN.024).

Appendix A. Supplementary data

Supplementary data to this article can be found online at https://doi.org/10.1016/j.microc.2021.106666.

References

[1] M. Nomachi, T. Kubo, K. Hosoya, K. Kaya, Solvent effects in the preparation of molecularly imprinted polymers for melatonin using N-propionyl- 5-

methoxytryptamine as the pseudo template, Anal. Bioanal. Chem. 384 (6) (2006) 1291–1296, https://doi.org/10.1007/s00216-006-0310-z.
[2] G. Chen, Y. Huo, D.X. Tan, Z. Liang, W. Zhang, Y. Zhang, Melatonin in Chinise medicinal herbs, Life Sci. 73 (2003) 19–26, https://doi.org/10.1016/s0024-3205(03)00252-2.
[3] R.J. Retter, M.L. Pablos, T.T. Agapito, J.M. Guerrero, Melatonin in the context of the free radical theory of aging, Ann. New York Acade. Sci. 786 (1996) 362–378, https://doi.org/10.1111/nyas.1996.786.issue-110.1111/j.1749-6632.1996.tb39077.x.
[4] R.J. Reiter, Oxidative damage in the central nervous system: protection by melatonin, Prog. Neurobiol. 56 (3) (1998) 359–384, https://doi.org/10.1016/S0301-0082(98)00052-5.
[5] M. Karbownik, R.J. Reiter, Antioxidative Effects of Melatonin in Protection Against Cellular Damage Caused by Ionizing Radiation, Proc. Soc. Exp. Biol. Med. 225 (1) (2000) 9–22, https://doi.org/10.1046/j.1525-1373.2000.22502.x.
[6] K. Celinski, P.J. Konturek, S. Konturek, M. Slomka, H. Cichoz-Lach, T. Brzozowski, et al., Effects of melatonin and tryptophan on healing of gastric and duodenal ulcers with helicobacter pylori infection in humans, J. Physiol. Pharmacol. 62 (5) (2011) 521–526, https://doi.org/10.1016/S0016-5085(12)61877-0.
[7] J. Jaworek, T. Brzozowski, S.J. Konturek., Melatonin as an organoprotector in the stomach and the pancreas, J. Pineal Res., 38 (2) (2005), 73-83, Doi: 10.1111/j.1600-079X.2004.00179.x.
[8] K. Ganguly, A.V. Sharma, R.J. Reiter, S. Swarnakar, Melatonin promotes angiogenesis during protection and healing of indomethacin-induced gastric ulcer: role of matrix metaloproteinase-2, J. Pineal Res. 49 (2) (2010) 130–140, https://doi.org/10.1111/j.1600-079X.2010.00776.x.
[9] M.H. Asghari, M. Moloudizargari, E. Ghobadi, M. Fallah, M. Abdollahi, Melatonin as a multifunctional anti-cancer molecule: Implications in gastric cancer, Life Sci. 185 (2017) 38–45, https://doi.org/10.1016/j.lfs.2017.07.020.
[10] S.R. Pandi-Perumal, A.S. BaHammam, G.M. Brown, D.W. Spence, V.K. Bharti, C. Kaur, R. Hardeland, D.P. Cardinali, Melatonin antioxidative defense: therapeutical implications for aging and neurodegenerative processes, Neurotox. Res. 23 (3) (2013) 267–300, https://doi.org/10.1007/s12640-012-9337-4.
[11] Y.-H. Wu, D.F. Swaab, The human pineal gland and melatonin in aging and Alzheimer's disease, J. Pineal Res. 38 (3) (2005) 145–152, https://doi.org/10.1111/jpi.2005.38.issue-310.1111/j.1600-079X.2004.00196.x.
[12] T. Lekic, R. Hartman, H. Rojas, A. Manaenko, W. Chen, R. Ayer, J. Tang, J. H. Zhang, Protective effect of melatonin upon neuropathology, striatal function, and memory ability after intracerebral hemorrhage in rats, J. Neurotrauma 27 (3) (2010) 627–637, https://doi.org/10.1089/neu.2009.1163.
[13] U. KOCA ÇALIŞKAN, C. AKA, E. BOR, Melatonin in Edible and Non-Edible Plants, Turk. J. Pharmaceut. Sci. 14 (1) (2017) 75–83, https://doi.org/10.4274/tjps10.4274/tjps.33043.
[14] S. Fraser, P. Cowen, M. Franklin, C. Franey, J. Arendt, Direct radioimmunoassay for melatonin in plasma, Clin. Chem. 29 (2) (1983) 396–397, https://doi.org/10.1093/CLINCHEM/29.2.396.
[15] Y. Li, V.M. Cassone, A simple, specific high-throughput enzyme-linked immunosorbent assay (ELISA) for quantitative determination of melatonin in cell culture medium, Int. Immunopharmacol. 28 (1) (2015) 230–234, https://doi.org/10.1016/j.intimp.2015.06.012.
[16] E.A. de Almeida, P. Di Mascio, T. Harumi, D. Warren Spence, A. Moscovitch, R. Hardeland, D.P. Cardinali, G.M. Brown, S.R. Pandi-Perumal, Measurement of melatonin in body fluids: Standards, protocols and procedures, Child's Nervous Syst. 27 (6) (2011) 879–891, https://doi.org/10.1007/s00381-010-1278-8.
[17] W. Sieghart, E. Ronca, G. Drexler, S. Karall, Improved radioimmunoassay of melatonin in serum, Clin. Chem. 33 (1987) 604–605, https://doi.org/10.1093/clinchem/33.4.604.
[18] M. Plebani, A.R. Masiero, M.L. Burlina, M.L. Chiozza, M. Scanarini, A. Burlina, Measurement of melatonin in blood by radioimmunoassay, Childs Nerv. Syst. 6 (1990) 220–221, https://doi.org/10.1007/BF01850977.
[19] B. Chegini, A. Ehrhart-Hofmann, A. Kaider, F. Waldhauser, Direct enzyme-linked immunosorbent assay and a radioimmunoassay for melatonin compared, Clin. Chem. 41 (1995) 381–386, https://doi.org/10.1093/clinchem/41.3.381.
[20] J.F. Peniston-Bird, W. Di, C.A. Street, A. Kadva, M.A. Stalteri, R.E. Silman, HPLC Assay Of Melatonın In Plasma Wıth Fluorescence Detectıon, Clin. Chem. 39 (1993) 2242–2247, https://doi.org/10.1093/clinchem/39.11.2242.
[21] A.F. Carneiro, C.N. Carneiro, F.J.V. Gomez, A. Spisso, M.F. Silva, L.A.C. Minho, W. N.L. dos Santos, F.d.S. Dias, Doehlert matrix for the optimization of ultrasound dispersive liquid–liquid microextraction of melatonin in Argentine and Brazilian wine samples, Microchem. J. 159 (2020) 105313, https://doi.org/10.1016/j.microc.2020.105313.
[22] F.J.V. Gomez, I.G. Hernández, S. Cerutti, M.F. Silva, Solid phase extraction/cyclodextrin-modified micellar electrokinetic chromatography for the analysis of melatonin and related indole compounds in plants, Microchem. J. 123 (2015) 22–27, https://doi.org/10.1016/j.microc.2015.05.013.
[23] E. Olad, M. Mohamad, T. Shamspur, A. Mostafavi, Spectrofluorimetric determination of melatonin in kernels of four different Pistacia varieties after ultrasound-assisted solid–liquid extraction, Spectrochim. Acta Part A Mol. Biomol. Spectrosc. 132 (2014) 326–329, https://doi.org/10.1016/j.saa.2014.05.010.
[24] W. Setyaningsih, E. Duros, M. Palma, C.G. Barroso, Optimization of the ultrasound-assisted extraction of melatonin fromred rice (Oryza sativa) grains through a response surface methodology, Appl. Acoust. 103 (2016) 129–135, https://doi.org/10.1016/j.apacoust.2015.04.001.
[25] S. Römsing, J. Ulfberg, Y. Bergqvist, Determination of melatonin in human plasma with solid-phase extraction, high-performance liquid chromatography and fluorescence detection, Scand. J. Clin. Lab. Invest. 63 (1) (2003) 81–88, https://doi.org/10.1080/00365510310000529.
[26] G. Simonin, L. Bru, E. Lelièvre, J.-P. Jeanniot, N. Bromet, B. Walther, C. Boursier-Neyret, Neyret, Determination of melatonin in biological fluids in the presence of the melatonin agonist S 20098: comparison of immunological techniques and GC-MS methods, J. Pharm. Biomed. Anal. 21 (3) (1999) 591–601, https://doi.org/10.1016/S0731-7085(99)00150-8.
[27] C. He, Y. Long, J. Pan, K. Li, F. Liu, Application of molecularly imprinted polymers to solid-phase extraction of analytes from real samples, J. Biochem. Bioph. Methods 70 (2) (2007) 133–150, https://doi.org/10.1016/j.jbbm.2006.07.005.
[28] C. He, F. Liu, K. Li, H. Liu, Molecularly imprinted polymer film grafted from porous silica for selective recognition of testosterone, Anal. Lett. 39 (2) (2006) 275–286, https://doi.org/10.1080/00032710500476946.
[29] H.-H. Yang, S.-Q. Zhang, F. Tan, Z.-X. Zhuang, X.-R. Wang, Surface molecularly imprinted nanowires for biorecognition, J. Am. Chem. Soc. 127 (5) (2005) 1378–1379, https://doi.org/10.1021/ja046762210.1021/ja0467622.s001.
[30] M. Glad, O. Norlow, B. Sellergren, N. Siegbahn, K. Mosbach, Use of silane monomers for molecular imprinting and enzyme entrapment in polysiloxanecoated porous silica, J. Chromatogr. A 347 (2000) 11–23, https://doi.org/10.1016/S0021-9673(01)95465-2.
[31] M.M. Sanagi, S. Salleh, W.A.W. Ibrahim, A.A. Naim, D. Hermawan, M. Miskam, I. Hussain, H.Y. Aboul-Enein, Molecularly imprinted polymer solid-phase extraction for the analysis of organophosphorus pesticides in fruit samples, J. Food Compos. Anal. 32 (2) (2013) 155–161, https://doi.org/10.1016/j.jfca.2013.09.001.
[32] H. He, M. Lin, Z. Han, Y. Muroya, H. Kudo, Y. Katsumura, The formation and properties of the melatonin radical: a photolysis study of melatonin with 248 nm laser light, Org. Biomol. Chem. 3 (2005) 1568–1574, https://doi.org/10.1039/B501202C.
[33] A.Z. Roldán, S.C. Avendaño, R.S. Montes, M.P. Pardavé, M.R. Romo, M.T.R. Silva, New insights on the spectrophotometric determination of melatonin pKa values and melatonin-βCD inclusion complex formation constant, Spectrochim. Acta Part A Mol. Biomol. Spectrosc. 190 (2018) 442–449, https://doi.org/10.1016/j.saa.2017.09.042.
[34] N.E. Moussaoui, A.E. Hassane, A. Bendriss, Melatonin stability at different storage conditions and during the ultrasound assisted extraction, International Journal of Current Research 7 (5) (2015) 15526–15530.
[35] N. M. Moussaoui, A. Bendriss, Analysis of Melatonin by High Performance Liquid Chromatography after Solid-Phase Extraction (SPE/HPLC-FD), Int. J. Eng. Res. Technol. (IJERT), 4 (2) (2015), 988-993, IJERT V4 020736.
[36] T. Rosado, I. Henriques, E. Gallardo, A.P. Duarte, Determination of melatonin levels in different cherry cultivars by high-performance liquid chromatography coupled to electrochemical detection, Eur. Food Res. Technol. 243 (10) (2017) 1749–1757, https://doi.org/10.1007/s00217-017-2880-8.
[37] L.G. Martins, N.M. khalil, R.M. Mainardes, Application of a validated HPLC-PDA method for the determination of melatonin content and its release from poly (lactic acid) nanoparticles, J. Pharm. Anal. 7 (6) (2017) 388–393, https://doi.org/10.1016/j.jpha.2017.05.007.
[38] J. Niu, X. Zhang, P. Qin, Y. Yang, S. Tian, H. Yang, M. Lu, Simultaneous Determination of Melatonin, L-Tryptophan, and two L-Tryptophan-Derived Esters in Food by HPLC with Graphene Oxide/SiO2 Nanocomposite as the Adsorbent, Food Anal. Methods 11 (9) (2018) 2438–2446, https://doi.org/10.1007/s12161-018-1213-2.